Journal of Materials Chemistry C

Accepted Manuscript

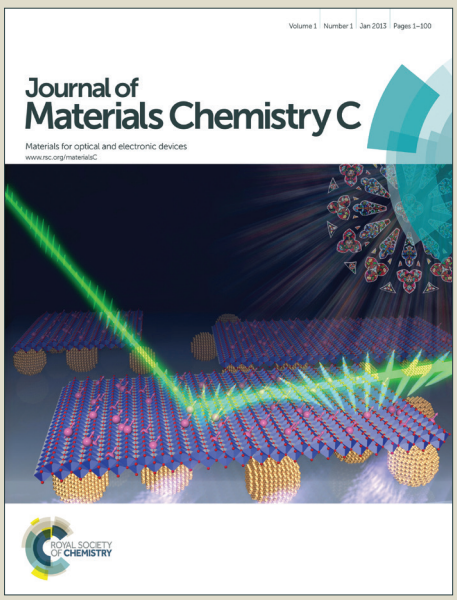

ROYAL SOCIETY OF CHEMISTRY

www.rsc.org/materialsC

Cite this: DOI: 10.1039/c0xx00000x

www.rsc.org/xxxxxx

ARTICLE TYPE

A water/alcohol-soluble copolymer based on fluorene and perylene diimide as a cathode interlayer for inverted polymer solar cells

Zhenfeng Zhao,[ab] Jiebing He,[a] Jiuxing Wang,[b] Weichao Chen,[b] Ning Wang,[b] Yong Zhang*[a] and Renqiang Yang*[b]

Received (in XXX, XXX) Xth XXXXXXXXX 20XX, Accepted Xth XXXXXXXXX 20XX

DOI: 10.1039/b000000x

A novel copolymer based on fluorene and perylene diimide with pendent amino groups, namely poly[2,9-bis(3-(dimethylamino)propyl)-5-methyl-12-(7-methyl-9,9-dioctyl-9H-fluoren-2-yl)anthra(2,1,9-*def*:6,5,10-*d'e'f'*)diisoquinoline-1,3,8,10(2H,9H)-tetraone] (PF-PDIN), has been synthesized and developed as a cathode interlayer for inverted polymer solar cells (I-PSCs). The PF-PDIN shows good alcohol solubility and uniform film morphology. The device with the configuration of ITO/PF-PDIN/P3HT:$PC_{61}BM$/MoO_3/Ag exhibits a power conversion efficiency (PCE) of 3.54 %. The resulting device shows higher efficiency and better stability relative to the device using organic small-molecular analogy, 2,9-bis(3-(dimethylamino)propyl)anthrax(2,1,9-*def*:6,5,10-*d'e'f'*)diisoquinoline-1,3,8,10(2H,9H)-tetraone (PDIN), as the cathode interlayer. This work indicates that PF-PDIN is a new promising candidate cathode interlayer for highly efficient and stable PSCs.

Introduction

Polymer solar cells (PSCs) have attracted much attention due to their potential application in flexible, lightweight, and large–area devices through low-cost solution processing.[1-6] Over the past several years, PSCs based on nanoscale phase separated blend of semiconducting conjugated polymer electron donor and fullerene derivative electron acceptor have shown a remarkable breakthrough. The highest reported power conversion efficiency (PCE) has exceeded 9.2 % for single solar cells[7] and 10 % for tandem solar cells.[8] PSCs have two main types of device structure, which are the conventional structure (ITO substrate/hole transport layer/active layer/electron transport layer/metal electrode) and inverted structure (ITO substrate/ electron transport layer/active layer/ hole transport layer /metal electrode).[9] In the conventional structure, their instability, particularly in the presence of oxygen and moisture, becomes a critical issue for real commercial applications because the active layer is normally sandwiched between transparent indium tin oxide (ITO), and low work function metals (normally Ca/Al), which are very chemically active in air. Compared to conventional PSCs, inverted PSCs (I-PSCs) have attracted increasing attention because of their greatly improved device stability by using air stable metals as the hole collecting electrode and ITO as the electron collecting electrode.[10] Unfortunately, the I-PSCs fabricated with a bare ITO cathode exhibit inferior performance because not only the high W_F of the ITO cathode (-4.7 eV) hinders the ohmic contact with the lowest unoccupied molecular orbital (LUMO) of the fullerene, reducing the open-circuit voltage (V_{oc}),[11, 12] but also the organic active layers have poor contact with the inorganic ITO cathode, which will result in low fill factor (FF) and short circuit current (J_{sc}). Therefore, in order to improve the PCE and stability of PSCs, finding some solution-processed organic interlayer inserted between the ITO and the photoactive layer becomes an important issue to PSCs.

Many materials such as zinc oxide (ZnO),[13, 14] titanium oxide (TiO_x),[15] MoO_3-Al composite,[16] cesium carbonate (Cs_2CO_3),[17, 18] water-soluble poly(ethylene oxide) (PEO),[19] and alcohol soluble fullerene derivatives[9, 20-24] used as cathode interlayers have successfully enhanced the PCE of PSCs. In those interlayers, water/alcohol-soluble organic or polymeric materials have advantages compared to inorganic interlayers due to their simple, vacuum-free and environment-friendly procedure to form a film during the device fabrication. Moreover, most of inorganic layers are sensitive to the UV-irradiation and the surface adsorption of oxygen.[25] To overcome the disadvantages of inorganic interfacial layers, we need to develop the promising candidates for the interlayer of PSCs. The organic polymeric/molecular interface materials require the introduction of specific functional groups (such as ethylene oxide,[26] phosphonate,[24, 27] amino or ammonium,[7, 28-32] etc.) that can form the desired interfacial dipole with the ITO substrate, thus reducing the W_F of ITO and significantly improving the charge transport and collection efficiency. Especially, perylene diimide-based interfacial materials have attracted great attention due to its several fascinating properties, such as photochemical stability, high electron affinities, easy functionalization and high conductivities.[28, 33-38] As we known, PDIN as an organic small-molecule is one of the most attractive reported cathode interfacial materials in organic solar cells. Despite the enhancement in the PCE, the device has a lower stability due to its strong crystalline, which renders the using of this material for a long time. Moreover, PDIN as an organic small-molecule has bad film formation, which limits its application. Therefore, finding some organic polymeric interface materials which have good film formation are necessary. Especially, fluorene-based interfacial materials have attracted great attention. As we known, poly[(9,9-bis(3'-(*N*,*N*-dimethylamino)propyl)-2,7-fluorene)-*alt*-2,7-(9,9–ioctylfluorene)] (PFN) as a water/alcohol-soluble conjugated polymer is one of the most attractive reported cathode interfacial materials in organic solar cells.[7, 39] The excellent electron extraction originated from the pinning Fermi level and the additional interface electric field are believed to contribute to the enhanced efficiency of the I-PSCs employing PFN as the cathode interfacial layer.[39]

Herein, based on the good performances of fluorene and perylene diimide, we synthesized a water/alcohol-soluble conjugated polymer PF-PDIN named poly[2,9-bis(3-(dimethylamino)propyl)-5-methyl-12-(7-methyl-9,9-dioctyl-9H-fluoren-2-yl)anthrax(2,1,9-*def*:6,5,10-*d'e'f'*)diisoquinoline-1,3,8,10(2H,9H)-tetraone]. PF-PDIN has good film formation, and good electron transport and collection properties. Most importantly, PF-PDIN can improve the PCE in I-PSCs with the device architecture of ITO/PF-PDIN/P3HT:$PC_{61}BM$/MoO_3/Ag where P3HT represents poly(3-hexylthiophene). For comparison, the reference devices with/without PDIN were made under the same conditions. Prominent PCEs as high as 3.54 % were achieved, which were much higher than those of the reference devices (2.99 %/1.95 %).

Experimental section

Materials and measurements

3,4,9,10-Perylenetetracarboxylic dianhydride (PDA) and 5,12-dibromoanthra[2,1,9-*def*:6,5,10-*d'e'f'*]diisochromene-1,3,8,10-tetraone (2BrPDA) were purchased from HWRK Chem and used without further purification. Fluorene was obtained from ENERGY CHEMICAL. Tetrakis(triphenylphosphine)palladium $(Pd(PPh_3))_4$ was purchased from Alfa Aesar. Poly(3-hexylthiophene) (P3HT) and [6,6]-phenyl-C_{61}-butyric acid methyl ester ($PC_{61}BM$) were purchased from American Dye Sources (ADS). Patterned ITO glass with a sheet resistance of 15 Ω per square was obtained from Shenzhen Display (China). Solvents were carefully dried and distilled from appropriate drying agents prior to use. All reactions were monitored by using thin-layer chromatography (TLC) with Merck pre-coated glass plates. Compounds were visualized with UV-light irradiation at 254 and 365 nm. ^1H and ^{13}C NMR spectra were measured in $CDCl_3$ on a Bruker AVANCE 600 HMz Fourier transform NMR spectrometer; chemical shifts were quoted relative to the internal standard tetramethylsilane. High resolution mass spectra (HRMS) were obtained using a Bruker Maxis UHR-TOF, Ion Source: APCI system. The absorption spectra were measured using a Hitachi U-4100 UV-Vis-NIR scanning spectrophotometer. The molecular weight of the polymer was measured by the gel permeation chromatography (GPC) performed using an ELEOS System, and polystyrene was used as the standard (room temperature, tetrahydrofuran (THF) as the eluent). Cyclic voltammetry (CV) measurements were performed on a CHI660D electrochemical workstation. The work station is equipped with a three-electrode cell consisting of a platinum working electrode, a saturated calomel electrode (SCE) reference electrode and a platinum wire counter electrode. The measurements were carried out in anhydrous acetonitrile containing 0.1 M n-Bu_4NPF_6 as a supporting electrolyte under argon atmosphere at a scan rate of 100 mV/s. Thin films were deposited from chloroform solution onto the working electrodes. The redox potential of the Fc/Fc+ internal reference is 0.38 V vs. SCE. The highest occupied molecular orbit (HOMO) and the lowest unoccupied molecular orbit (LUMO) energy levels were determined by calculating the empirical formula[40] of E_{HOMO}=-e(E_{ox}+4.8-$E_{1/2}^{(Fc/Fc+)}$), E_{LUMO}=-e(E_{red}+4.8-$E_{1/2}^{(Fc/Fc+)}$), where E_{ox} and E_{red} were the onset oxidation and reduction potential, respectively. Atomic force microscope (AFM) images were acquired with Agilent-5400 scanning probe microscope with a Nanodrive controller in tapping mode with MikroMasch NSC-15 AFM tips with resonant frequencies of ~300 kHz. Thermo gravimetric analysis (TGA) measurement was performed by a SDT Q600 V20.9 Build 20 at a heating rate of 10 °C/min.

Synthesis

5,12-dibromo-2,9-bis(3-(dimethylamino)propyl)anthra[2,1,9-*def*:6,5,10-*d'e'f'*]diisoquinoline-1,3,8,10(2H,9H)-tetraone (2). Monomer **1** (1.0 g, 1.82 mmol) in 36ml tert-Butanol was sonicated for 10min. *N*,*N*-dimethyl-1,3-propanediamine (1.25 ml, 10.05 mmol) was added and the reaction mixture was stirred at 130 ℃ for 24 h under nitrogen. Upon water addition, a red solid was precipitated. The red solid was separated by filtration, washed repeatedly with water and was further purified by column chromatography (silica gel; CH_2Cl_2:triethylamine, 50:1 v/v). The product was dried under vacuum to provide 2BrPDIN as a red solid (yield=46%, 0.6 g). ^{1}HNMR (600 MHz, $CDCl_3$): δ (ppm) 9.48 (dd, 2H), 8.92 (d, 2H), 8.70 (dd, 2H), 4.27 (m, 4H), 2.45 (t, 4H), 2.26 (m, 12H), 1.93 (m, 4H). MS (UHR-TOF): calcd. for $C_{34}H_{30}Br_2N_4O_4$ $[M]^+$, 716.0634; found, 716.0630.

Poly[2,9-bis(3-(dimethylamino)propyl)-5-methyl-12-(7-methyl-9,9-dioctyl-9H-fluoren-2-yl)anthrax(2,1,9-*def*:6,5,10-*d'e'f'*)diisoquinoline-1,3,8,10(2H,9H)-tetraone] (PF-PDIN). Monomer **3** (128.5 mg, 0.2 mmol) and monomer **2** (143.7 mg, 0.2 mmol) were dissolved in a mixture of toluene (5 ml), 2 M aqueous solution of Na_2CO_3 (0.8 ml) and some droups of Aliquant336. The reaction container was purged with N_2 for 30 min to remove O_2. $Pd(PPh_3)_4$ (11.5 mg) was added and the mixture was heated under reflux for 48h. Then, the mixture was cooled to room temperature and the polymer was precipitated in CH_3OH. The precipitates were collected by filtration, and then washed with MeOH and hexane. The solid was dissolved in $CHCl_3$ and passed through a column packed with alumina, celite and silica gel. The column as eluted with $CHCl_3$. The combined polymer solution was concentrated, and was poured into MeOH, after which, the precipitate was collected and dried under vacuum overnight. Yield: 104.4 mg (55%). The number-average molecular weight (M_n) was 11.2 KDa, polydispersity index (PDI) was 2.16. ^{1}HNMR (600 MHz, $CDCl_3$): δ (ppm) 8.74 (br, 2H), 7.80-7.31 (m, 10H), 4.20 (br, 4H), 3.91-2.20 (br, 20H), 2.05-1.49 (m, 34H).

Fabrication and characterization of PSCs

Fabrication of PSCs: The PSCs were fabricated as an inverted photovoltaic device architecture, ITO/cathode interlayer/P3HT:$PC_{61}BM$/MoO_3/Ag. Firstly, ITO coated glass substrates were ultrasonically cleaned sequentially in detergent, water, acetone, and isopropyl alcohol. PF-PDIN (1.5 mg mL^{-1}) and PDIN (1.5 mg mL^{-1}) were dissolved in methanol under the presence of a small amount of acetic acid. Then, the PF-PDIN or PDIN was spin-cast onto the ITO substrates with the speed at 2000 rpm. The active layer was then spin-coated onto the cathode interlayer (P3HT/$PC_{61}BM$ = 1 : 1 with a total concentration of 18 mg mL^{-1} in dichlorobenzene (DCB)) with the addition of DIO at 800 rpm. Finally, a thin layer of MoO_3 (3 nm) and Ag (80 nm) were thermal evaporated under 2.0×10^{-4} Pa to complete the inverted structure. As for comparison, the devices without a buffer layer were made under the same conditions. The effective area of a single device was 0.15 cm^2.

The PCEs of the inverted solar cell devices were measured under an AM 1.5G solar simulator (Oriel model 91160). The photo and dark current density-voltage (*J-V*) characteristics were recorded with Keithley 2400 source measurement unit under simulated 100 mW cm^{-2} irradiation from a Newport solar simulator. The external quantum efficiencies (EQEs) of solar cells were analyzed using a certified Newport incident photon conversion efficiency (IPCE) measurement system.

Table 1 Physicochemical property of the PF-PDIN-interlayer.

	UV-vis absorption spectra			Cyclic voltammetry		
	Solution	Film				
Interlayer	λ_{max} /nm	λ_{max} /nm	E_g^{opt} /eV	HOMO (eV)	LUMO (eV)	E_g^{EC}/eV
PDIN[a]	465/480/530	480/555	2.03	-6.05	-3.72	2.33
PF-PDIN	300/462/552	305/466/552	1.74	-5.51	-3.83	1.68

[a] the data was from the reference reported.[28]

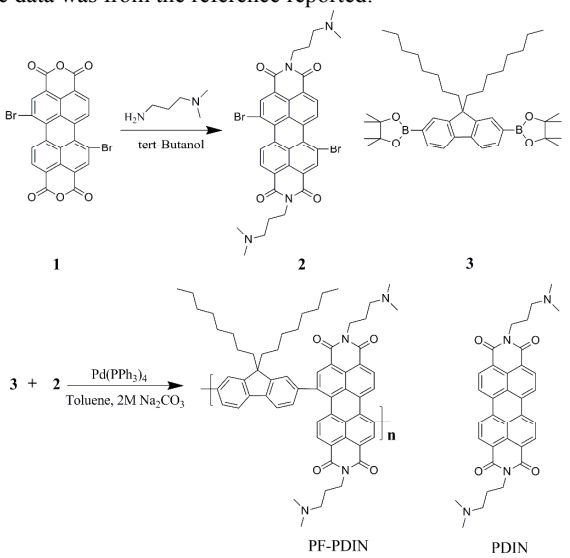

Scheme 1. Chemical structure and synthetic route of PF-PDIN.

Results and discussion

Material synthesis

The synthetic route of PF-PDIN is shown in Scheme 1. 2,7-bis(4,4,5,5-tetramethyl-1,3,2-dioxaborolan-2-yl)-9,9-dioctylfluorene (3)[41, 42] was prepared according to the published procedures. The purity of monomer 2 was 85% for the existence of its isomer and they were difficult to separate. PF-PDIN based on monomer 2 and monomer 3 was synthesized by Suzuki coupling reaction. PDIN has been synthesized according to the reported paper.[28] PF-PDIN has poor solubility in $CHCl_3$.

Thermal stability

The TGA measurement of PF-PDIN is shown in Fig. 1. PF-PDIN shows good thermal stability and possesses high decomposition temperature (T_d), ranging from 250-292 °C.

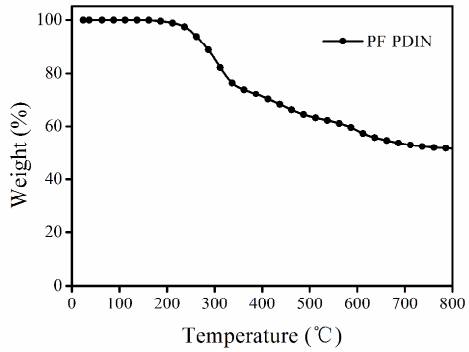

Fig. 1 TGA characteristic of PF-PDIN.

Physicochemical properties

Polymer PF-PDIN is alcohol soluble, while it needs the assistance of acetic acid (4 ‰ in volume). However, it has poor solubility in chlorobenzene and dichlorobenzene, which is very important for inverted device fabrication. Its absorption spectra and cyclic voltammogram are provided in Fig. 2 and physicochemical property is collected in Table 1. PF-PDIN showed three absorption peaks in solution, which was similar to other reported PDI-based polymers.[43] The absorption spectra of the films were not notably red-shifted compared with those in solution, indicating that little intermolecular interaction occurred in the solid state, probably due to the large steric hindrance of the many bulky side chains. From the cyclic voltammogram, the onset reduction potential (E_{on}^{red}) and onset oxidation potential (E_{on}^{ox}) were evaluated to be -0.58, -1.10 V for PF-PDIN. The reference electrode was calibrated by the ferrocene/ferrocenium (Fc/Fc+) (4.8 eV below vacuum level)[43] to obtain accurate energy levels. The LUMO levels of PF-PDIN was thus calculated to be -3.83 eV. The LUMO was very close to those of $PC_{61}BM$ (about -3.71 eV), which could smoothly bridge electrons to transport from the fullerene acceptor to the cathode side.[28] The HOMO energy levels of PF-PDIN was estimated to be -5.51 eV. In addition, the Kelvin probe results shows the W_F of ITO coated by PF-PDIN was reduced from 4.70 eV for pure ITO to 3.85 eV by using a KP 6500 Digital Kelvin probe (McAllister Technical Services. Co. Ltd).

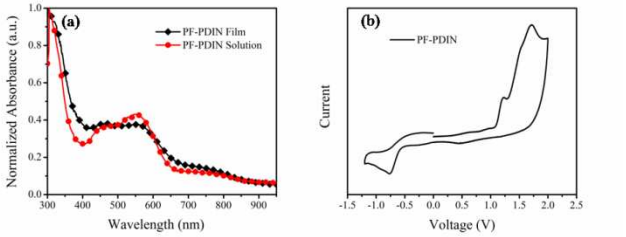

Fig. 2 UV–vis absorption and electrochemical properties of PF-PDIN. (a) Absorption spectra in 0.045 mg mL^{-1} $CHCl_3$ solution and in film state. (b) Cyclic voltammogram of the PF-PDIN.

Photovoltaic performance

I-PSCs were fabricated with the configuration of ITO/PF-PDIN /P3HT:$PC_{61}BM$/MoO_3/Ag to study the interfacial function of PF-PDIN. In this inverted device structure, ITO was used as the cathode, MoO_3/Ag as the anode, P3HT and $PC_{61}BM$ used as the donor and acceptor, respectively. The chemical structure of P3HT and $PC_{61}BM$, the device configuration, and the energy levels of the corresponding materials in the devices are presented in Scheme 2. PF-PDIN from its alcohol solution was deposited on the top of ITO as an interlayer. For comparison, control devices with/without PDIN as the cathode interlayer were also fabricated under the same conditions.

The current density-voltage (*J-V*) curves for the I-PSCs measured under AM 1.5 G irradiation (100 mW cm^{-2}) are presented in Fig. 3 and the corresponding device characteristics including a short-circuit current density (J_{sc}), open circuit voltage (V_{oc}), fill factor (FF), power conversion efficiency (PCE) values, Shunt resistance (R_{sh}), and series resistance (R_s) are summarized in Table 2. I-PSC with a bare ITO electrode performed poor with a PCE of 1.94 %, a V_{oc} of 0.53 V, a J_{sc} of 8.92 mA cm^{-2}, and a FF

of 41 %. After inserting a thin interlayer of PDIN, the PCE of the device reached 2.99 % with a significantly enhanced FF of 58 %, a fairly improved V_{oc} of 0.56 V and J_{sc} of 9.21 mA cm^{-2}. Interestingly, the device with PF-PDIN as the cathode interlayer delivered comparable performance as the device using PDIN as the interlayer. The PF-PDIN/ITO electrode device showed a higher PCE of 3.54 %, with a V_{oc} of 0.60, a J_{sc} of 9.52 mA cm^{-2} and a FF of 62 %. Notably, V_{oc}, J_{sc} and FF of the device with PF-PDIN as the cathode interlayer were simultaneously enhanced relative to the bare ITO electrode device, which led to higher overall performance. It is interesting that PF-PDIN exhibited comparable performance as an cathode interlayer material relative to PDIN, making it a good alternative cathode interlayer material in I-PSC device design.

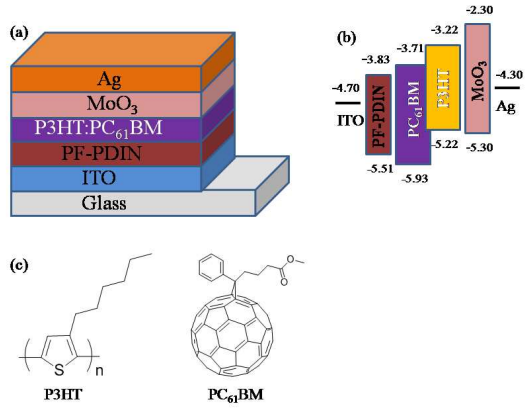

Scheme 2. (a) Device structure of I-PSCs using PF-PDIN as interlayer. (b) Energy level diagram of the component materials used in device fabrication (unit: eV). (c) Chemical structures of P3HT and $PC_{61}BM$.

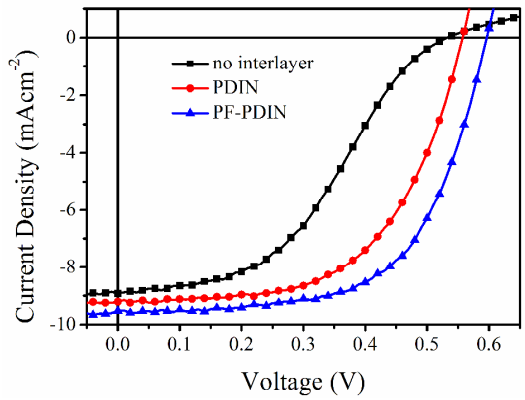

Fig. 3 *J-V* characteristics of the I-PSCs without interlayer and with PDIN or PF-PDIN interlayer.

Table 2 Device parameters of the I-PSCs based on P3HT/$PC_{61}BM$ as the active layers without interlayer and with PDIN or PF-PDIN interlayer under the illumination of AM 1.5G, 100 mW cm^{-2}.

Interlayer	V_{oc} (V)	J_{sc} (mA cm^{-2})	FF (%)	PCE (%)	R_{sh}[a] (kΩ cm^2)	R_s[b] (Ω cm^2)
No	0.53	8.92	41	1.94	0.35	18.22
PDIN	0.56	9.21	58	2.99	4.01	11.02
PF-PDIN	0.60	9.52	62	3.54	6.21	9.21

[a] Calculated from the inverse slope at $V = 0$ in *J-V* curves under illumination. [b] Calculated from the inverse slope at $V = V_{oc}$ in *J-V* curves under illumination.[44, 45]

To further scrutinize the electrical characteristics of the PF-PDIN-based interlayer in inverted devices, the dark *J-V* characteristics were measured (Fig. 4). In the regime of -0.50 to 0.68 V, the reverse and leakage currents of the device with the cathode interlayer of PF-PDIN and PDIN was suppressed compared to that of the bare ITO electrode device. It has been reported that the reduced reverse dark current contributed to the V_{oc} enhancement by incorporating WSCPs as the cathode interlayers in PSCs.[30, 46] Meanwhile, such reduced dark leakage current is also beneficial for PCE improvements in PSC devices.[47] While in the region over 0.68 V, the devices with PDIN and PF-PDIN as a interlayer showed higher injection currents compared to that of the bare ITO electrode, which is indicative of increased electron injection from the ITO electrode and is consistent with the decreased R_s (18.22, 11.02, and 9.21 Ω cm^2 for the bare ITO, PDIN/ITO and PF-PDIN/ITO devices, respectively) (see Table 2).[24] The increased V_{oc} could be attributed to the interface dipoles generated by PF-PDIN, and the increased electric field could improve charge transport properties, eliminate the build-up of space charge and reduce recombination loss,[48] leading to increased J_{sc} and FF.[49]

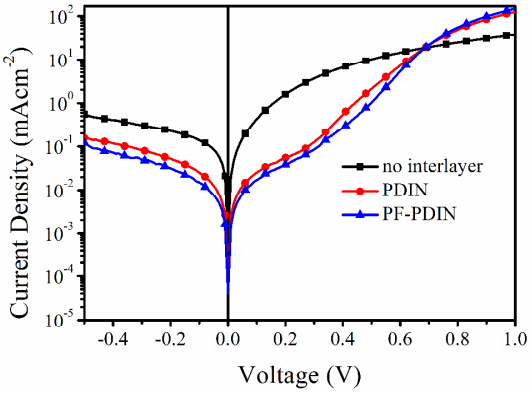

Fig. 4 dark *J-V* characteristics of the I-PSCs without interlayer and with PDIN or PF-PDIN interlayer.

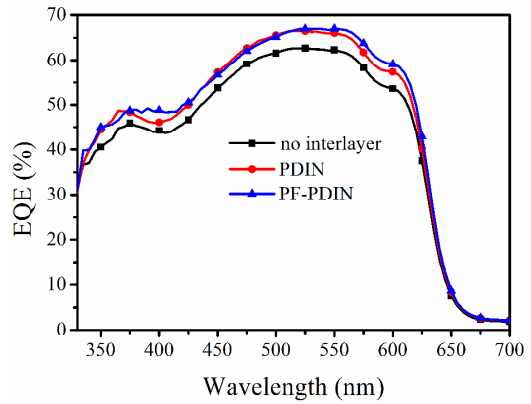

Fig. 5 EQE spectra of the I-PSCs without interlayer and with PDIN or PF-PDIN interlayer.

To gain an further understanding of the improvement of device performance after inserting the PF-PDIN cathode interlayer, the external quantum efficiency (EQE) spectra (see Fig. 5) of the I-PSCs both with and without interlayer were measured. With different cathode interlayer, the shape of the EQE curve of the devices were almost identical across the entire wavelength range. In addition, it is seen that the ITO/PF-PDIN device shows the highest EQE value, which is consistent with the value obtained from *J–V* curves.

The ability of adjusting the morphology of the interlayer is very important for optimizing device performance, since the ohmic contact between the active layer and ITO electrode is strongly dependent on the morphology of the interlayer in devices. So atomic force microscope (AFM) under the tapping mode was used to track the surface morphologies of PDIN and PF-PDIN interlayer on the ITO substrates. As comparison, the surface morphologies of ITO without a interlayer were measured by AFM. The corresponding images were presented in Fig. 6. The root-mean-square (RMS) roughness of bare ITO surface was 0.80 nm. By coating a thin PF-PDIN interlayer onto the ITO, the RMS roughness value was 0.88 nm, which indicated that PF-PDIN had a good film forming property. Correspondingly, the RMS roughness of the ITO/PDIN layer increased to 1.38 nm due to the property of PDIN aggregating, which was much higher than those of the bare ITO and ITO/PF-PDIN films. The PF-PDIN interlayer showed a smooth and homogeneous morphology and can effectively prevent the leakage current at the interface between the active layer and ITO electrode, thus enhancing the efficiencies of the devices.

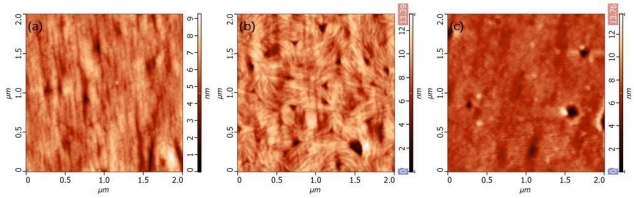

Fig. 6 AFM of (a) ITO glass, (b) PDIN-coated ITO, and (c) PF-PDIN-coated ITO.

To illustrate the solvent resistance of the PDIN and PF-PDIN thin films, UV-vis absorption spectra of the thin films were measured before and after washed by dichlorobenzene (DCB), and the UV-vis spectroscopy are shown in Fig. 7. It can be seen from Fig. 7 that the PDIN film was washed 58 % away, however, the PF-PDIN film was only washed 20 % away, which indicated that PF-PDIN has a better solvent resistance ability.

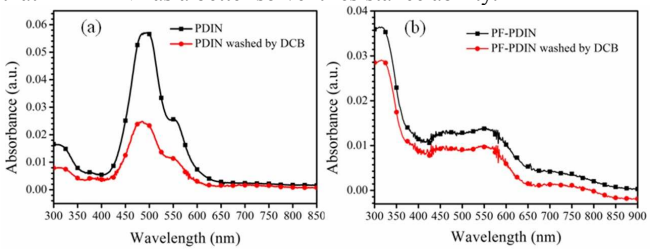

Fig. 7 UV-vis spectra of PDIN (a) and PF-PDIN (b) films before and after washing by DCB.

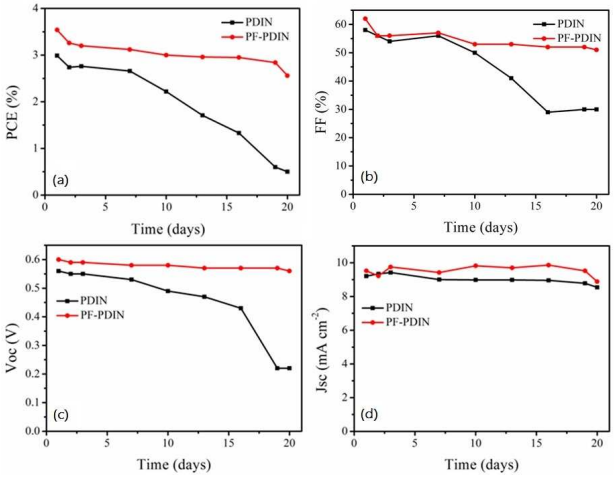

Fig. 8 Device performance of I-PSCs stored 20 days in nitrogen under ambient conditions. (a) PCE, (b) FF, (c) V_{oc}, and (d) J_{sc}, respectively.

These devices were stored in nitrogen at room temperature and periodically tested for 20 days to gauge the device stability [Fig. 8(a)-8(d)]. The device using PDIN as the cathode interlayer showed very unstable. PCE of the corresponding devices reduced with a rapid speed after seven day of storage and reached 0.5 % after twenty days. The rapid reduction of PCE should be contributed to the Characteristic of easy aggregation and ability of weak solvent resistance, which could be seen from Fig. 6(b) and Fig. 7(a). On the contrary, the device using PF-PDIN as the interlayer showed high stability. Both FF and V_{oc} over the period of 20 days remained relatively constant with the J_{sc} slightly decreasing over this time leading to PCE of over 75 %.

Conclusions

In conclusion, a water/alcohol soluble conjugated polymer PF-PDIN containing pendent amino groups was synthesized and employed as cathode interlayer for the I-PSCs. This new polymer demonstrates the properties necessary for an effective interface material including uniform film formation, good solvent resistance ability and excellent electron extraction. Compared to the device with PDIN as cathode interlayer, a simultaneous enhancement in V_{oc}, J_{sc} and FF of the I-PSCs with PF-PDIN as a cathode interlayer has been observed. As a result, the inverted device ITO/PF-PDIN/P3HT:$PC_{61}BM$/MoO_3/Ag showed a PCE of 3.54 %. It indicates that PF-PDIN is a new promising candidate as a good cathode interlayer for highly efficient and stable I-PSCs.

Acknowledgements

This work was supported by the Nature Science Foundation of China (U1174001, 61377065), the Science and Technology Planning Project of Guangdong Province (2012CB010200032), the Science and Technology Project of Guangzhou City (2012J2200023, 2014J4100056), and the Open Fund of the State Key Laboratory of Luminescent Materials and Devices (South China University of Technology)

Notes and references

[a]Guangdong Provincial Key Laboratory of Nanophotonic Functional Materials and Devices, Institute of Optoelectronic Material and Technology, South China Normal University, Guangzhou 510631, China. Tel: +86-20-85215603-807; Tel: +86-20-852114354; E-mail: zycq@scnu.edu.cn
[b]CAS Key laboratory of Bio-based Materials, Qingdao Institute of Bioenergy and Bioprocess Technology, Chinese Academy of Sciences, Qingdao 266101, China. Fax: +86-532-80662778; Tel: +86-532-80662700; E-mail: yangrq@qibebt.ac.cn

1. P. M. Beaujuge and J. M. J. Fréchet, *Journal of the American Chemical Society*, 2011, **133**, 20009-20029.
2. D. Demeter, T. Rousseau and J. Roncali, *RSC Advances*, 2013, **3**, 704-707.
3. J. Kim, H. M. Ko, N. Cho, S. Paek, J. K. Lee and J. Ko, *RSC Advances*, 2012, **2**, 2692-2695.
4. Y. Lin, Y. Wang, J. Wang, J. Hou, Y. Li, D. Zhu and X. Zhan, *Advanced Materials*, 2014, **26**, 5137-5142.
5. J. Yang, J. You, C.-C. Chen, W.-C. Hsu, H.-r. Tan, X. W. Zhang, Z. Hong and Y. Yang, *ACS Nano*, 2011, **5**, 6210-6217.
6. L. Han, X. Bao, T. Hu, Z. Du, W. Chen, D. Zhu, Q. Liu, M. Sun and R. Yang, *Macromolecular rapid communications*, 2014, **35**, 1153-1157.
7. Z. He, C. Zhong, S. Su, M. Xu, H. Wu and Y. Cao, *Nature Photonics*, 2012, **6**, 593-597.
8. J. You, L. Dou, K. Yoshimura, T. Kato, K. Ohya, T. Moriarty, K. Emery, C.-C. Chen, J. Gao and G. Li, *Nature communications*, 2013, **4**, 1446.
9. N. Wang, L. Sun, X. Zhang, X. Bao, W. Zheng and R. Yang, *RSC Advances*, 2014, **4**, 25886.
10. S. K. Hau, H.-L. Yip and A. K. Y. Jen, *Polymer Reviews*, 2010, **50**, 474-510.
11. L.-M. Chen, Z. Xu, Z. Hong and Y. Yang, *Journal of Materials Chemistry*, 2010, **20**, 2575-2598.
12. H.-L. Yip and A. K.-Y. Jen, *Energy & Environmental Science*, 2012, **5**, 5994-6011.
13. T. Stubhan, H. Oh, L. Pinna, J. Krantz, I. Litzov and C. J. Brabec, *Organic Electronics*, 2011, **12**, 1539-1543.
14. Y. Sun, J. H. Seo, C. J. Takacs, J. Seifter and A. J. Heeger, *Advanced Materials*, 2011, **23**, 1679-1683.
15. C. Waldauf, M. Morana, P. Denk, P. Schilinsky, K. Coakley, S. Choulis and C. Brabec, *Applied Physics Letters*, 2006, **89**, 233517.
16. J. Liu, S. Shao, G. Fang, B. Meng, Z. Xie and L. Wang, *Adv Mater*, 2012, **24**, 2774-2779.
17. H.-H. Liao, L.-M. Chen, Z. Xu, G. Li and Y. Yang, *Applied Physics Letters*, 2008, **92**, 173303-173303-173303.
18. G. Li, C.-W. Chu, V. Shrotriya, J. Huang and Y. Yang, *Applied Physics Letters*, 2006, **88**, 253503-253503-253503.
19. F. Zhang, M. Ceder and O. Inganäs, *Advanced Materials*, 2007, **19**, 1835-1838.
20. W. Jiao, D. Ma, M. Lv, W. Chen, H. Wang, J. Zhu, M. Lei and X. Chen, *Journal of Materials Chemistry A*, 2014, **2**, 14720-14728.
21. S. Li, M. Lei, M. Lv, S. E. Watkins, Z. a. Tan, J. Zhu, J. Hou, X. Chen and Y. Li, *Advanced Energy Materials*, 2013, **3**, 1569-1574.
22. X. Li, W. Zhang, Y. Wu, C. Min and J. Fang, *Journal of Materials Chemistry A*, 2013, **1**, 12413-12416.
23. Q. Mei, C. Li, X. Gong, H. Lu, E. Jin, C. Du, Z. Lu, L. Jiang, X. Meng and C. Wang, *ACS applied materials & interfaces*, 2013, **5**, 8076-8080.
24. C. Duan, C. Zhong, C. Liu, F. Huang and Y. Cao, *Chemistry of Materials*, 2012, **24**, 1682-1689.
25. N. Cho, H.-L. Yip, S. K. Hau, K.-S. Chen, T.-W. Kim, J. A. Davies, D. F. Zeigler and A. K. Y. Jen, *Journal of Materials Chemistry*, 2011, **21**, 6956.
26. Y. Zhou, F. Li, S. Barrau, W. Tian, O. Inganäs and F. Zhang, *Solar Energy Materials and Solar Cells*, 2009, **93**, 497-500.
27. J. Sun, Y. Zhu, X. Xu, L. Lan, L. Zhang, P. Cai, J. Chen, J. Peng and Y. Cao, *The Journal of Physical Chemistry C*, 2012, **116**, 14188-14198.
28. Z.-G. Zhang, B. Qi, Z. Jin, D. Chi, Z. Qi, Y. Li and J. Wang, *Energy & Environmental Science*, 2014, **7**, 1966.
29. Y. Zhou, C. Fuentes-Hernandez, J. Shim, J. Meyer, A. J. Giordano, H. Li, P. Winget, T. Papadopoulos, H. Cheun, J. Kim, M. Fenoll, A. Dindar, W. Haske, E. Najafabadi, T. M. Khan, H. Sojoudi, S. Barlow, S. Graham, J. L. Bredas, S. R. Marder, A. Kahn and B. Kippelen, *Science*, 2012, **336**, 327-332.
30. T. Yang, M. Wang, C. Duan, X. Hu, L. Huang, J. Peng, F. Huang and X. Gong, *Energy & Environmental Science*, 2012, **5**, 8208.
31. S. Liu, Z. Zhang, D. Chen, C. Duan, J. Lu, J. Zhang, F. Huang, S. Su, J. Chen and Y. Cao, *Science China Chemistry*, 2013, **56**, 1119-1128.
32. S. Liu, K. Zhang, J. Lu, J. Zhang, H. L. Yip, F. Huang and Y. Cao, *J Am Chem Soc*, 2013, **135**, 15326-15329.
33. F. Nolde, W. Pisula, S. Müller, C. Kohl and K. Müllen, *Chemistry of Materials*, 2006, **18**, 3715-3725.
34. L. Chen, C. Li and K. Müllen, *Journal of Materials Chemistry C*, 2014, **2**, 1938.
35. F. Wurthner, *Chemical communications*, 2004, 1564-1579.
36. C. Huang, S. Barlow and S. R. Marder, *The Journal of organic chemistry*, 2011, **76**, 2386-2407.
37. W. Yue, A. Lv, J. Gao, W. Jiang, L. Hao, C. Li, Y. Li, L. E. Polander, S. Barlow, W. Hu, S. Di Motta, F. Negri, S. R. Marder and Z. Wang, *J Am Chem Soc*, 2012, **134**, 5770-5773.
38. Y. Zhang, L. Chen, K. Zhang, H. Wang and Y. Xiao, *Chemistry*, 2014, **20**, 10170-10178.
39. S. Zhong, R. Wang, H. Ying Mao, Z. He, H. Wu, W. Chen and Y. Cao, *Journal of Applied Physics*, 2013, **114**, 113709.
40. G. Zhang, F.-I. Wu, X. Jiang, P. Sun and C.-H. Cheng, *Synthetic Metals*, 2010, **160**, 1906-1911.
41. M. Ranger, D. Rondeau and M. Leclerc, *Macromolecules*, 1997, **30**, 7686-7691.
42. R. Yang, R. Tian, Q. Hou, W. Yang and Y. Cao, *Macromolecules*, 2003, **36**, 7453-7460.
43. E. Zhou, K. Tajima, C. Yang and K. Hashimoto, *Journal of Materials Chemistry*, 2010, **20**, 2362-2368.

44. Z.-G. Zhang, H. Li, Z. Qi, Z. Jin, G. Liu, J. Hou, Y. Li and J. Wang, *Applied Physics Letters*, 2013, **102**, 143902.
45. Z.-G. Zhang, H. Li, B. Qi, D. Chi, Z. Jin, Z. Qi, J. Hou, Y. Li and J. Wang, *Journal of Materials Chemistry A*, 2013, **1**, 9624.
46. C. He, C. Zhong, H. Wu, R. Yang, W. Yang, F. Huang, G. C. Bazan and Y. Cao, *Journal of Materials Chemistry*, 2010, **20**, 2617.
47. N. Li, B. E. Lassiter, R. R. Lunt, G. Wei and S. R. Forrest, *Applied Physics Letters*, 2009, **94**, 023307.
48. Z. He, C. Zhong, X. Huang, W. Y. Wong, H. Wu, L. Chen, S. Su and Y. Cao, *Adv Mater*, 2011, **23**, 4636-4643.
49. V. D. Mihailetchi, L. J. A. Koster and P. W. M. Blom, *Applied Physics Letters*, 2004, **85**, 970.